Thermal expansion responses of pressure infiltrated SiC/Al metal-matrix composites

S. ELOMARI*
Spacecraft Engineering, Canadian Space Agency, Saint-Hubert, J3Y 8Y9, Canada

R. BOUKHILI
Department of Mechanical Engineering, Montreal Polytechnic School, Montreal, Canada

C. SAN MARCHI, A. MORTENSEN
Department of Materials Science and Engineering, Massachusetts Institute of Technology, Cambridge, MA, USA

D.J. LLOYD
Alcan International Limited, Kingston Research and Development Centre, Kingston, ON, Canada

Aluminium–matrix composites containing thermally oxidized and unoxidized SiC particles featuring four average particle diameters ranging from 3 to 40 μm were produced by vacuum assisted high pressure infiltration. Their thermal expansion coefficient (CTE) was measured between 25 and 500 °C. Oxidation of the SiC particles in air produces the formation at their surface of silicon oxide in quantities sufficient to bond the particles together, and confer strength to preforms. After infiltration with pure aluminium, the composites produced showed no sign of significant interfacial reaction. The CTE of the composite reinforced with unoxidized SiC particles featured an abrupt upward deviation upon heat-up near 200 °C, and a second abrupt decrease near 400 °C. The first transition is attributed to an inversion of stress across particle contact points. When composites are produced with oxidized SiC particles, these two transitions were removed, their CTE varying smoothly and gradually from the lower elastic bound to the upper elastic bound as temperature increases. With both composite types, the CTE decreased as the average particle size decreased. This work illustrates the benefits of three-dimensional reinforcement continuity for the production of low-CTE metal matrix composites, and shows a simple method for producing such composites.

1. Introduction

Advanced composites show considerable promise for applications where weight and volume are critical as, for example, in aircraft and space vehicles. Among the various systems that have been explored, cast composites of an aluminium-based matrix reinforced with SiC and Al_2O_3 particles show particular engineering potential because of their comparatively low fabrication costs. These composites provide, compared with the unreinforced metal, significant improvements in elastic modulus [1–4], wear resistance [5], fatigue resistance [6], damping capacity [7], and high-temperature mechanical properties [8, 9]. Furthermore, compared with unreinforced metals, ceramic particle reinforced aluminium can feature a low thermal expansion, that can be tailored by varying the volume fraction and morphology of the ceramic phase [10]. This last attribute, combined with the high thermal conductivity of aluminium–matrix composites and their low density, renders this class of composites particularly attractive as materials for applications such as electronic heat sinks and space structures. As a result, such composites are currently considered as a replacement for conventional metals used in electronic packaging applications, such as Cu, Al, Ni–Fe alloys, and Cu–W and Cu–Mo blends.

The composite system most usually considered for this class of applications is silicon carbide particle reinforced aluminium. The SiC particulates, which are available in different structures, are produced from inexpensive raw materials, exhibit low density ($d = 3.2\ \mathrm{g\,cm^{-3}}$), low thermal expansion coefficient (CTE) ($\alpha = 4.7 \times 10^{-6}\ \mathrm{K^{-1}}$), and a high Young's modulus ($E = 450$ GPa). Commercially available particle sizes range from 1 to 80 μm. The thermal conductivity, k, of SiC is in the range 80 to 200 $\mathrm{W\,m^{-1}\,K^{-1}}$,

* Visiting Scientist at Massachusetts Institute of Technology.

0022–2461

depending on purity and processing conditions. By contrast, pure Al has the following physical properties: $d = 2.7\,\mathrm{g\,cm^{-3}}$, $E = 70\,\mathrm{GPa}$, $\alpha = 23 \times 10^{-6}\,\mathrm{K^{-1}}$, and $k = 180$ to $230\,\mathrm{W\,m^{-1}\,K^{-1}}$. The CTE of Al–10% Si alloys with 55 to 75 vol% SiC reinforcement thus falls in the range 6.4 to $9.2 \times 10^{-6}\,\mathrm{K^{-1}}$ [11, 12]; these values approach the CTE of electronic materials such as Si ($4.1 \times 10^{-6}\,\mathrm{K^{-1}}$) or gallium arsenide ($5.8 \times 10^{-6}\,\mathrm{K^{-1}}$). Several low cost manufacturing techniques have been developed toward the production of high-volume fraction composites in this system; these include powder metallurgy processing, gas-pressure driven infiltration, centrifugal casting, and squeeze casting. Among these fabrication methods, the squeeze casting technique appears to be one of the more effective in that it is well suited for mass production, and is a comparatively simple process for manufacturing near-net-shape composites of relatively complex geometry.

In an earlier article [13], the influence of reinforcement architecture was explored towards the minimization of composite CTE for a fixed volume fraction of reinforcement. It was found that the internal reinforcement architecture does exert an influence on composite thermal expansion, but only after matrix plastification, and in a manner not predicted by straightforward theory. The observed composite expansion behaviour was explained as being a result of internal stresses, and of the presence of very small volume fractions porosity, both natural consequences of the fabrication process used to produce these composites, namely pressure infiltration. In that earlier work, the reinforcement architecture was varied by comparing SiC particle reinforced aluminium with a SiC microcellular foam reinforced aluminium composite. The reinforcing phase of this latter composite was produced via a process developed at MIT, which produces fine microcellular foams of high microstructural integrity, but which is also relatively complex.

In this work we explore an alternative, and more economical, method of varying the level of internal connectivity of the SiC reinforcing phase; we bond the SiC particles by simple oxidation in air at elevated temperature. As will be shown, this produces a film of silica along the particle surface, which fuses these partially together, conferring some level of tensile strength to the preform.

In what follows, we present a comparison of composites having a matrix of pure aluminium, containing oxidized and unoxidized SiC reinforcements ranging from 3 to 40 μm in size. We first describe the processing of these composites, then we discuss the thermal expansion behaviour of the two types of infiltrated composites produced, and its agreement with continuum mechanical models.

2. Experimental procedures

2.1. Materials and fabrication of preforms

The matrix was 99.9% initial purity aluminium from ALCOA™ (Trademark, Aluminium Company of America, Pittsburgh, PA, USA). Four SiC particulates from two suppliers and with average diameters in the range 3 to 40 μm were used; these are given in Table 1. Preforms 30 mm thick were produced by first packing SiC particles by hand into a boat made of Fiberfrax™ board. Stirring of the particles with an impeller was performed to improve particle distribution uniformity. Oxidation of the particles was carried out in air, under programmed heating and with an isothermal hold at 1300 °C. The temperature in the hot zone was kept constant to within 1 °C. As the preforms used in this study were fabricated using different particle sizes, the oxidation time was varied somewhat, ranging from two to four hours.

2.2. Metal-matrix composites production

Preforms were infiltrated with pure aluminium using the squeeze casting press shown in Fig. 1. The apparatus consists of a steel die containing a cylinder in which a steel piston travels. The piston is centred above the cylinder with a steel ring. The interior of the cylinder was lined with a tube of graphite foil and fiberfrax™ insulation. Pressure is provided by an RC-1010 Enerpac hydraulic ram. A vacuum line at the bottom of the die permits application of a vacuum to the preform during infiltration.

In each composite infiltration experiment, the preform and the aluminium were heated separately to 800 °C. The procedure consisted of dropping a boat made of fiberfrax™ containing the preform into the die preheated to 250 °C; then, the aluminium was immediately poured over it. The piston was inserted into the die, and the vacuum and pressure simultaneously applied. The molten metal was infiltrated into the preform under 34 MPa. The relatively cold die resulted in rapid cooling of the metal, and the composite was therefore rapidly solidified under pressure. Details of the casting procedures were varied somewhat, depending on reinforcement preform cohesion, and depending on whether or not the SiC particles were oxidized.

The composite samples were cut along their length on a low-speed diamond saw, using ethanol as a lubricant. Metallography was performed by first grinding

TABLE I Some characteristics of the SiC particulates used in this work. The suppliers are also reported

Type	Purity (%)	Size (μm)	Supplier
Green	99.9	3	Norton (Worcester, MA, USA)
Black	98.7	10	Tech-Met Canada (Scarborough, Ontario, Canada)
Black	98.7	20	–
Black	98.7	40	–

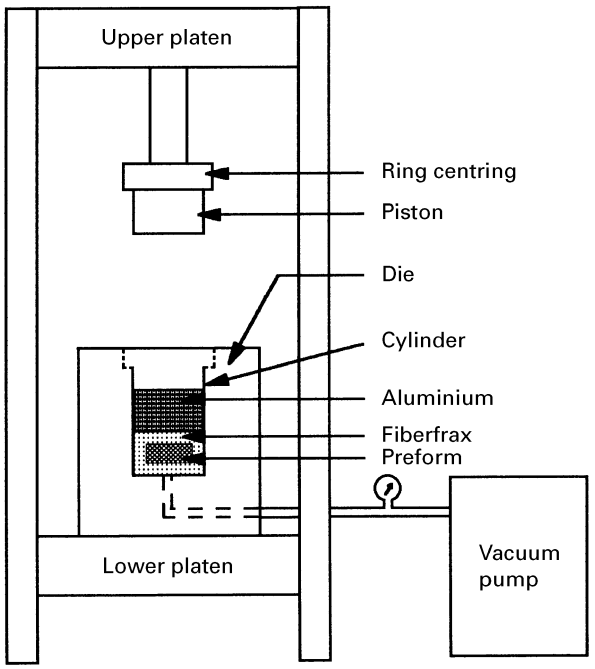

Figure 1 Schematic of the pressure infiltration unit.

the samples with a 200 grit perforated diamond wheel. Samples were then polished using 15 μm, 6 μm, and 3 μm Buehler Metadi™ (Lake Bluff, IL, USA) diamond suspensions on Buehler Metlap 10™ spiral polishing platens. Samples were washed with water and ethanol between polishing steps. Finally, samples were polished for approximately 10 min on Buehler Chemomet™ polishing cloth using Buehler Mastermet™ polishing compound. Scanning electron microscope examination of the polished composite was performed on a Jeol 840 microscope equipped with energy dispersive X-ray analysis. The volume fractions of the SiC particles were measured using an IBAS2 image analyser system attached to an optical microscope.

2.3. Measurement of thermal expansion

CTE measurements were performed from 25 to 500 °C at 5 °C min^{-1} using a commercial thermo-mechanical analysis equipment (model TMA 2940, Dupont de Nemours). The thicknesses of the samples were measured with increased sensitivity (0.1 μm) using the standard expansion probe. Specimens for CTE testing, $10 \times 5 \times 2$ mm in size, were machined from the cast metal-matrix composites (MMC) samples. Specimen surfaces were polished using 1 μm diamond paste. More than four samples of each composite were tested under each condition to verify reproducibility of the data. In each test, the sample was positioned on a quartz stage and a moveable probe was placed on the top of the sample. The thermal expansion of the specimen was detected by a linear variable differential transformer (LVDT) attached to the probe during heating and cooling, provided by a furnace surrounding both the sample stage and the probe. The sample temperature was measured using a thermocouple adjacent to the sample. Data were obtained in the form of curves of PLC (per cent linear change) versus temperature. TMA standard data analysis software was used to derive the coefficient of thermal expansion of the composites tested from these data.

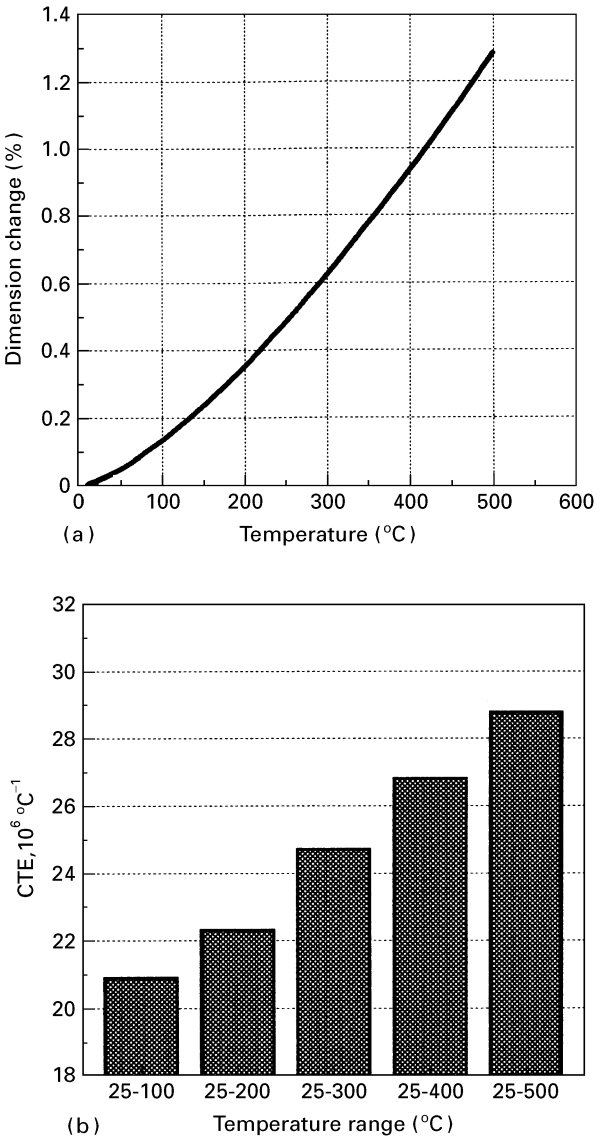

Figure 2 Thermal expansion of pure aluminium: (a) dimension changes, and (b) thermal expansion coefficient versus temperature range.

In order to test the reliability of the CTE measurements, a pure aluminium sample (99.9%) was also evaluated. Its mean CTE between 25 and 300 °C was measured as 24.8×10^{-6} °C^{-1} as shown in Fig. 2. This value compares well with that of 25.3×10^{-6} °C^{-1} quoted in the literature for pure aluminium between room temperature and 300 °C [14]. All composite samples were cycled twice from 25 to 500 °C to detect any early effect of thermal cycling.

3. Results

3.1. Microstructural characterization

Silicon carbide particles were examined in the scanning electron microscope (SEM), both in the as-received condition and after oxidation. As illustrated in Fig. 3, the preform before oxidation had "clean" particle surfaces free of clusters. After oxidation, it is

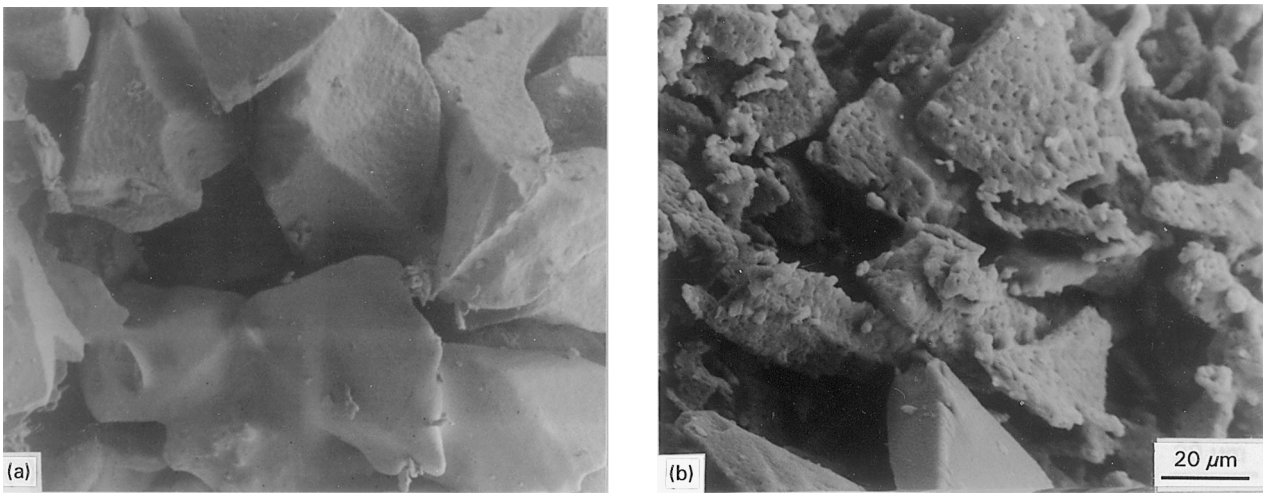

Figure 3 SEM micrographs of 40 μm SiC particles: (a) in as-received condition, and (b) after condition for 4 h in air at 1300 °C.

seen that the average particle size had increased, many of the particulates having been cemented together by the silica formed during oxidation. This glassy SiO_2 phase is clearly evident in Fig. 3(b), which shows the roughened appearance of the SiC particle surface after oxidation.

Figure 4 shows SEM micrographs of polished sections of the composites. Infiltration of the oxidized preforms produced composites in which most of the material appeared to be free of porosity and microscopically homogeneous (Fig. 4(a) and (b)). The preforms containing unoxidized SiC particles were also successfully infiltrated with pure aluminium (Fig. 4(c) and (d)); however, composites fabricated with the unoxidized particles were found to feature some localized regions containing pores of diameter comparable to

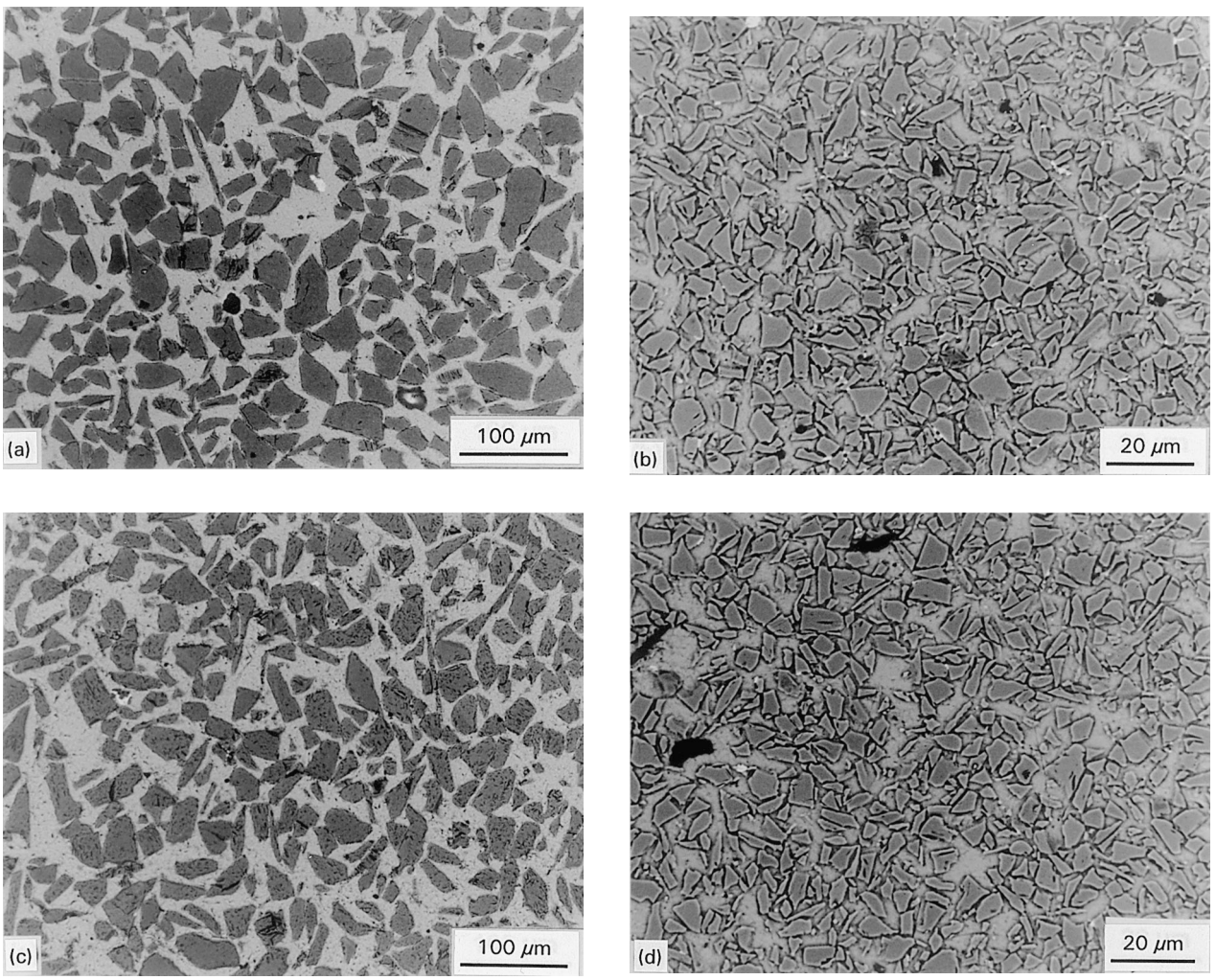

Figure 4 Microstructures of infiltrated SiC/Al metal–matrix composites: (a) oxidized 40 μm SiC particles, (b) oxidized 3 μm particles, (c) unoxidized 40 μm particles, and (d) unoxidized 3 μm particles.

TABLE II Image analysis results of infiltrated SiC/Al composites

Particle size (μm)	3	10	20	40
Oxidation				
SiC vol%	55	54	56	56
Porosity vol%	≈ 0	≈ 0	≈ 0	≈ 0
Without oxidation				
SiC vol %	46	48	48	48
Porosity vol %	2.2	1.8	2.3	2.0

that of the SiC particles (Fig. 4(d)). The oxidized preforms retained their shape in the final composite, in contrast with the unoxidized preforms which had undergone some compression, which was retained in the solidified composites.

There was no sign of interfacial reaction between the reinforcement and the matrix in either type of composite. Differential scanning calorimetry testing (DSC) combined with energy dispersive X-ray analysis in the SEM revealed no second phases either in the matrix, or near the matrix/reinforcement interfaces.

The volume fraction of silicon carbide in the composites was determined via image analysis; results are given in Table 2. The experimental uncertainty of these measurements is estimated to be about 2%; hence, the volume fraction is essentially constant within experimental error for each class of composite produced, at 55 and 47 % for oxidized and unoxidized composites, respectively. As expected, the volume fraction reinforcement is higher in composites produced from an oxidized preform. The average volume fraction of porosity found in the composites reinforced with unoxidized particles was 2 %. This value may be an overestimate, since some of the visible pores could have resulted from SiC fracture and removal during metallographic preparation.

3.2. Thermal expansion

The composite thermal expansion, expressed as per cent linear change (PLC), as a function of temperature, are shown in Figs 5 and 6 for composites containing oxidized and unoxidized SiC particulates, respectively. The thermal cycling experiments produced no conclusive evidence of thermal ratcheting in any of the materials during two cycles.

The PLC versus temperature curves for the unoxidized particle reinforced composites is somewhat more complex (Fig. 6). The first heat-up curves show two linear regions; the first, in the 25–200 °C range, has a lower slope than the subsequent, 200–300 °C

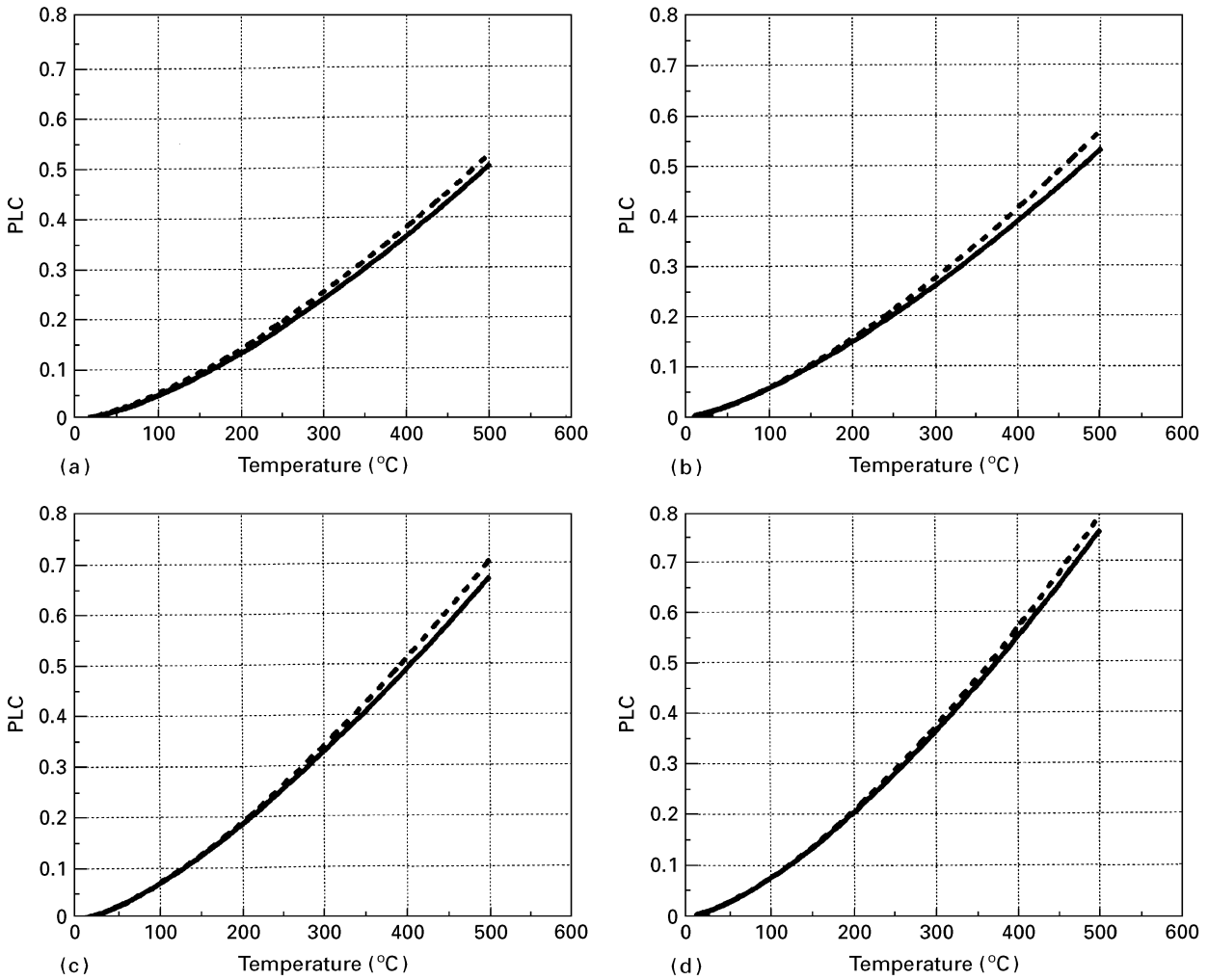

Figure 5 Per cent linear change (PLC) versus temperature for composites reinforced with various oxidized SiC particle sizes: (a) 3 μm, (b) 10 μm, (c) 20 μm, and (d) 40 μm. —— cycle 1; - - - - cycle 2.

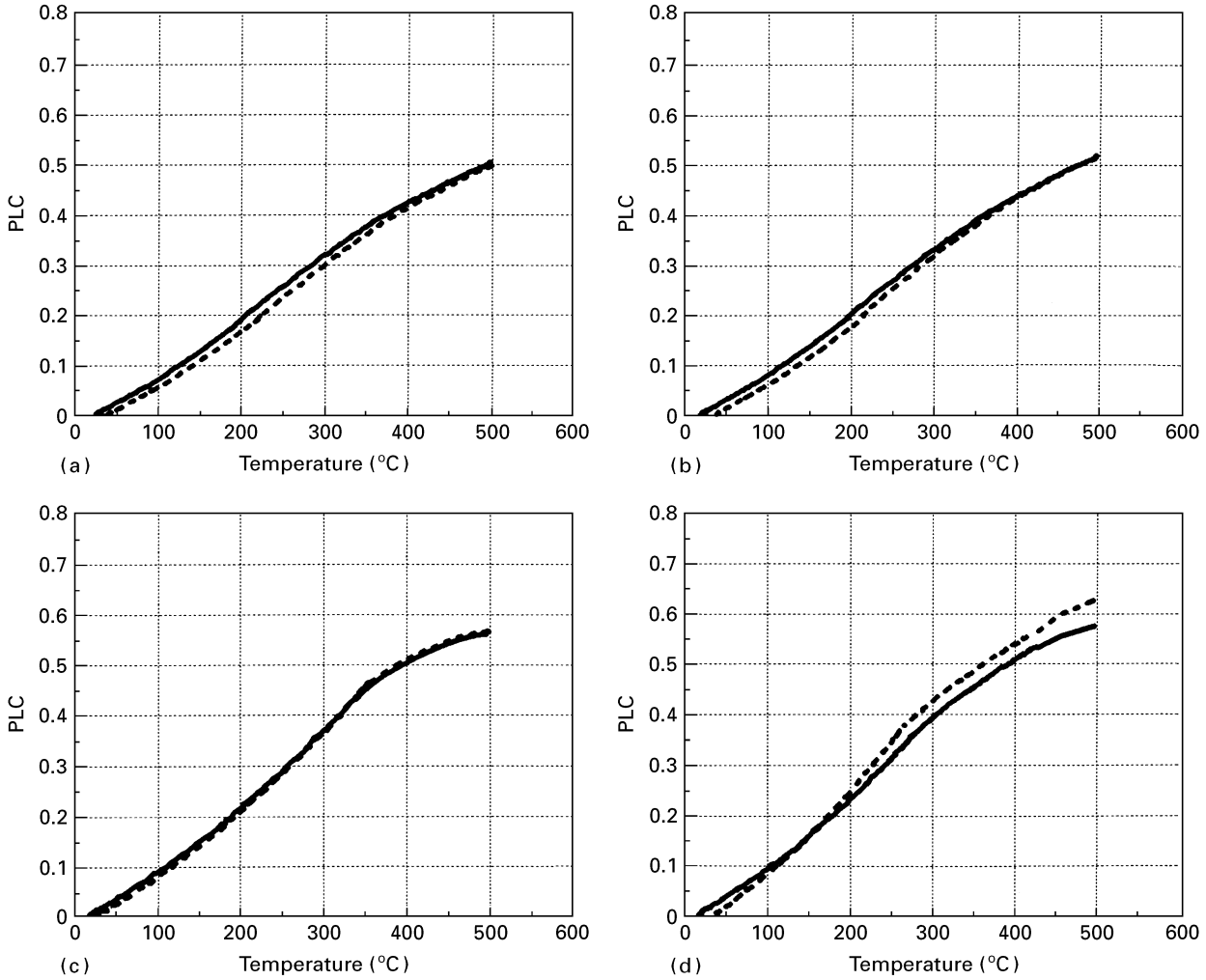

Figure 6 Per cent linear change (PLC) versus temperature for composites reinforced with various unoxidized SiC particle sizes: (a) 3 μm, (b) 10 μm, (c) 20 μm, and (d) 40 μm. —— cycle 1; - - - - cycle 2.

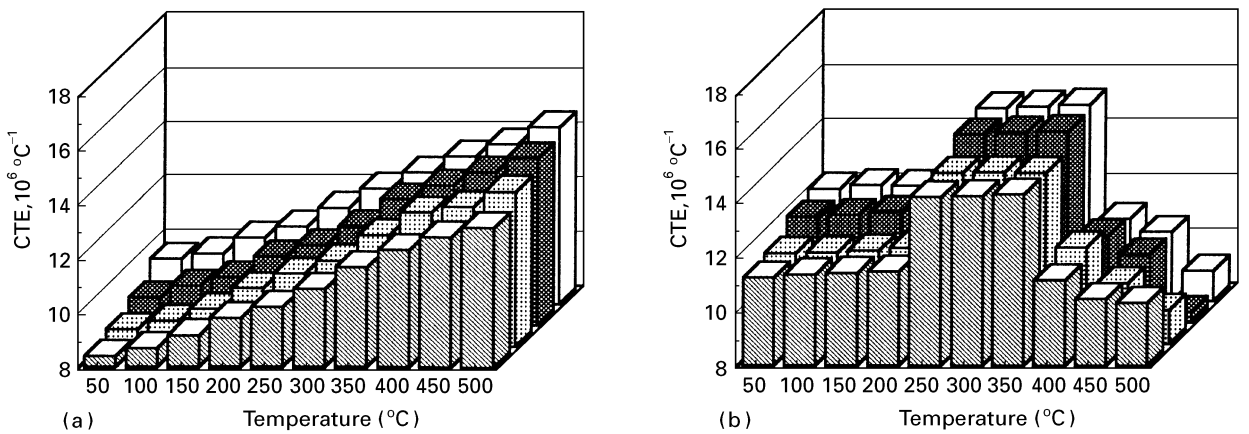

Figure 7 Coefficient of thermal expansion versus temperature for infiltrated composites: (a) with preform oxidation, and (b) without preform oxidation. ■3 μm; ▨10 μm; ▩20 μm; □40 μm.

region. These two regions are followed by a third region, in which the CTE again falls to a low level. In the second heat-up curve, the same regions with similar slopes are clearly seen.

As shown in Figs 5 and 6, there is an influence of particle size on the CTE of both composite types; the larger the particles are, the greater is the thermal expansion at a particular temperature. This effect is slightly less pronounced with the unoxidized particles.

Figure 7 shows the values of the coefficient of thermal expansion (CTE) as a function of temperature for each of the composites tested; the reported CTE values were determined at intervals of 50 °C based on the calculated slope fit between two selected temperatures. As expected from Fig. 5, the larger oxidized

particle reinforced composite shows a consistently higher average CTE than the composite containing smaller oxidized particles (Fig. 7a). It is evident that for a given initial volume fraction SiC and SiC particle size, the average CTE is decreased by the oxidation process. This is consistent with image analysis results, which indicate a higher volume fraction of the composite reinforcement with oxidized particles.

4. Discussion

4.1. Oxidation of the SiC particulates

The SEM micrographs for the oxidized SiC particles, as compared to those of unoxidized particulates, show that the SiC particles have been cemented together by the viscous silica glass formed by the oxidation reaction. Larger reinforcements (20–40 μm) exhibited little particle coalescence; in contrast, some fusion of the smaller particles (3 μm) was observed and SiO_2 droplets could be identified on many of the particle surfaces after oxidation at 1300 °C. The apparent silicon carbide particle size showed an increase, following this oxidation exposure, and clear evidence of bonding of the particles by the glassy silica phase. After oxidation at 1300 °C, even for periods of 2 h, particles 3 μm in size were found to have fused into a bonded network as a result of the flow of the silica glass from particle to particle.

Although the growth of a scale of SiO_2 is expected on silicon carbide during oxidation at elevated temperatures, the formation of a mobile film of silica at temperatures as low as 1300 °C is somewhat surprising since the melting point of silica is 1713 °C; however, according to Hummel [15], the presence of metastable forms of silica, such as high quartz or high tridymite, could lead to melting at considerably lower temperatures.

4.2. Microstructure of the SiC/AL composites

None of the composites showed any interfacial reaction. This is attributable to the low die temperature used in composite production combined with the rapidity of infiltration and solidification. The observed lack of interfacial reaction under the casting conditions used here is in agreement with the extensive literature on the Al/SiC system, reported in [16].

Microscopic observations combined with image analysis show that the composites containing oxidized particles are very homogeneous and have negligible porosity. In addition, the average volume fraction of oxidized particles is relatively high (55 vol % on average) compared to that of unoxidized reinforcement (47 vol % on average). These investigations are in good agreement with those carried out by Narciso *et al* [17] on the pressure infiltration of thermally oxidized SiC particulates by liquid aluminium; these authors reported that pre-oxidation of SiC particles decreased the threshold pressure for infiltration with aluminium by about 10 %. This decrease was attributed to changes in the specific surface area of the SiC preform.

4.3. Composite thermal expansion

4.3.1. Theoretical models of the CTE of isotropic composites

The CTE of a metal-matrix composite is relatively difficult to predict precisely because it is influenced by several factors. These include matrix plasticity and the internal structure of the composite, which typically consists of particles or fibres embedded in a continuous metallic matrix.

Composites produced in this work are random and isotropic. Despite the presence of a two-layer structure for the oxidized particles, we assume that both the matrix and the reinforcement phases can each be treated as a single homogeneous phase. It is also assumed that the interfacial shear strength at the interface is adequate to avoid interface failure. Given the nature and geometry of the phases present in these composites, both assumptions appear reasonable.

Several theoretical analyses have been presented in the literature which give expressions for the CTE of the metal-matrix composite; these are reviewed in [18–20]. If both phases of the composite only deform elastically, bounds on the composite CTE can be deduced from derived bounds for the modulus of isotropic composites [21]. Each of these bounds corresponds to the CTE of an elementary spherical composite featuring a sphere of one phase surrounded by a uniform layer of the other phase. With SiC as the central sphere in the model composite element, this upper bound corresponds to the model proposed earlier by Kerner for particle reinforced composites, given in [18–20]. The Kerner expression for the composite CTE, corresponding to the upper elastic bound derived by Schapery [21], is:

$$\alpha_C = V_P \alpha_P + V_m \alpha_m + \left[\frac{4G_m}{K_C}\right]\left[\frac{(K_C - K_P)(\alpha_m - \alpha_P) V_P}{4G_m + 3K_P}\right] \quad (1)$$

where α, V, G and K refer to CTE, volume fraction, shear modulus and bulk modulus, respectively, and subscripts m, p, and c stand for matrix, particle and composite, respectively. K_C is the bulk modulus of this composite (corresponding to Hashin and Strikhman's lower bound), given by:

$$K_C = \frac{\dfrac{V_P K_P}{3K_P + 4G_m} + \dfrac{V_m K_m}{3K_m + 4G_m}}{\dfrac{V_P}{3K_P + 4G_m} + \dfrac{V_m}{3K_m + 4G_m}} \quad (2)$$

Schapery's lower bound is calculated with the same formulae, after inversion of subscripts m and p.

A simpler model that is often used in the literature is the Turner model. This model assumes that each component in the composite is constrained to change dimensions with temperature changes at the same rate as the composite and that shear deformation is negligible. Writing that the stress in each phase is given by the product of volume strain and bulk modulus, and that internal stresses must balance to a zero volume-averaged sum, the following expression

is obtained:

$$\alpha_C = \frac{\alpha_p V_p K_p + \alpha_m V_m K_m}{V_p K_p + V_m K_m} \quad (3)$$

This expression falls below Schapery's lower bound for the CTE of elastic composites; it can not therefore be used rigorously for analysis of purely elastic composites.

In the presence of matrix plasticity, the composite apparent CTE will deviate from the bounds derived in Schapery's analysis of elastic composites. An extension of the Kerner model to include the influence of matrix plasticity, together with elementary physical reasoning, leads to the deductions that a composite of discrete elastic particles separated by a plastically deforming matrix will feature a CTE approaching the value predicted by the simple rule of mixtures expression (given by Equation 1 with the third term on its right-hand deleted) [22], whereas that of an Al–SiC composite featuring interconnected matrix and reinforcement phases should decrease somewhat towards the value predicted by the Turner equation [13].

We note that the composites were prepared at a temperature significantly above ambient. Differential shrinkage during cooldown from processing temperatures therefore will have resulted in the build-up of internal stresses, which are predominantly tensile in the matrix, and compressive in the SiC reinforcement; these pre-existing thermal stresses may also influence the composite CTE. We also note that, since all of these analyses are based on the use of continuum elasticity, the particle size does not appear in resulting expressions for the composite thermal expansion.

4.3.2. Thermal expansion of the composites

Results from CTE measurements conducted on the composites are plotted together with predictions from the four expressions given in the previous section in Fig. 8(a) for composites produced with the oxidized particle preforms, and in Fig. 8(b) for composites produced with SiC particles having undergone no oxidation treatment prior to the infiltration process. Predicted composite CTE values were calculated using measured values of the CTE of pure Al, Fig. 3(b) and data for other parameters given in [13, 14, 23], Table 3.

It is seen that the measured CTE shows, for each composite type, similar variations with temperature, but with a slight decrease in the CTE value, by about $10^{-6}\,K^{-1}$, as the SiC particle size decreases from 40 to 3 μm. This effect of particle size is not, as mentioned, predicted by mechanical models. Recently, Xu *et al.* [24] have examined the effect of reinforcement size on the CTE of TiC/Al XD^{TM} metal–matrix composite, in which the TiC particle sizes were 0.7 μm and 4.0 μm. These authors reported that the 4 μm particle composite showed, consistently, a higher CTE than the 0.7 μm particle reinforced composite. This was attributed to lattice distortion at the interfacial zone, where physical and/or mechanical interaction occurs. It is unlikely that, in the absence of matrix/particle coherency in the Al/SiC system, lattice distortion beyond what is predicted by continuum elasticity analysis would exist near the fibre/matrix interface of the composites investigated here; hence this explanation seems unlikely to apply to the present data. The apparent influence of reinforcement particle size on the CTE may reflect differences in the relative amount of silicon oxide present as the particle size varies; with a roughly constant silica layer thickness, smaller

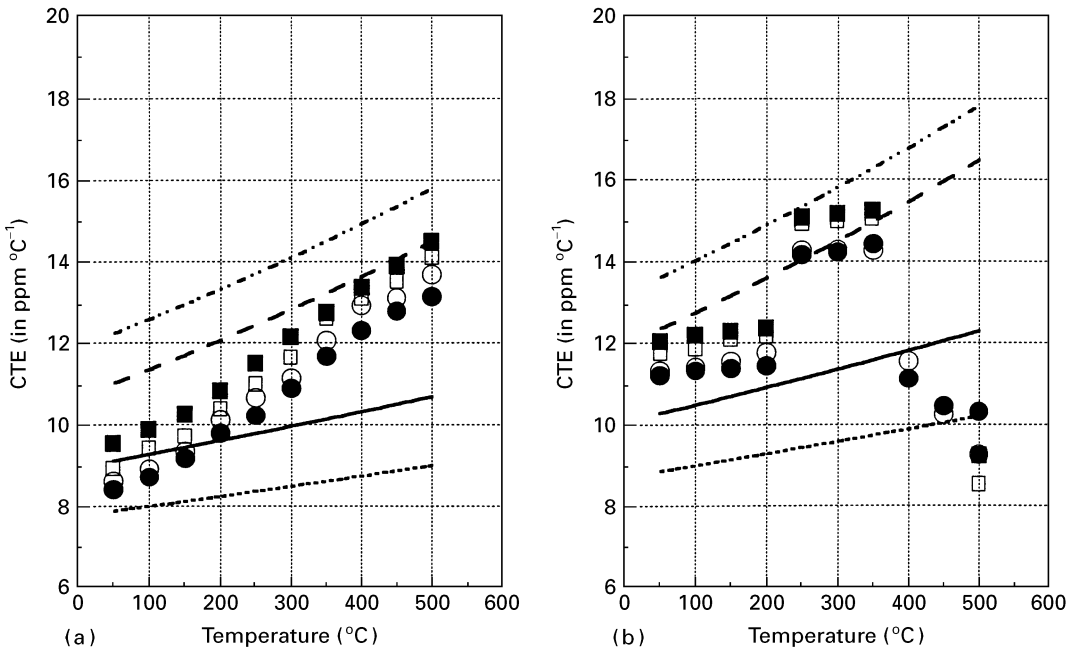

Figure 8 Comparison of the measured CTE of infiltrated SiC/Al composites with the theoretical predictions (Kerner's and Turner's) for infiltrated composites: (a) with preform oxidation, and (b) without preform oxidation. ● 3 μm; ○ 10 μm; □ 20 μm; ■ 40 μm. – –, Kerner; ——, Schap; - - - - Turner; —··— ROM.

TABLE III Properties of SiC and pure Al

T °C	SiC				Pure aluminum			
	E (GPa)	G (GPa)	K (GPa)	CTE (μ/°C)	E (GPa)	G (GPa)	K (GPa)	CTE (μ/°C)
50	450	192	227	4.5	72.03	27.2	68.28	21.8
100	450	192	227	4.5	70.66	26.6	68.55	22.4
200	450	192	227	4.5	65.90	24.7	66.21	23.9
300	450	192	227	4.5	63.73	24.1	59.79	25.9
400	450	192	227	4.5	49.16	18.1	60.96	27.8
500	450	192	227	4.5	36.91	13.2	60.48	29.5

particles will result in a higher silica content in the composite in proportion to the SiC. To evaluate the influence of this effect, the CTE of composites of aluminium reinforced with silica coated SiC was evaluated, assuming a silica CTE of $0.5 \times 10^{-6}\,°C^{-1}$. A silica layer with a thickness of 0.75 micrometres can account for the difference of $1.28 \times 10^{-6}\,°C^{-1}$ in the CTE at 50 °C, between composites containing 3 and 40 micrometre particles. This indicates that an oxide layer on the SiC particles may be giving rise to the apparent particle size effect in the CTE for oxidized preforms. However, this oxide thickness is much larger than the 20 Angstrom oxide layer typically present on unoxidized SiC, and cannot account for any particle size effect in unoxidized preforms.

Other possible explanations for a size effect of the particle on composite CTE, such as matrix alloying by interfacial reaction (which was not observed in metallography), or variations in volume fractions of SiC or porosity (which do not vary systematically with particle size, Table 2) do not seem to apply to the present composites either.

CTE values measured on composites produced from oxidized preforms show no significant departure from the predictions of elastic analysis, since these lie, overall, within the elastic bounds predicted by Schapery's analysis, Fig. 8(a). The variation of measured CTE with temperature exceeds that of predicted bounds; as temperature increases, composite CTE values cross the elastic CTE value field from the lower elastic bound towards the upper elastic bound. The behaviour of these interconnected composites thus differs at elevated temperature from that which was measured in [13] with pressure-infiltrated SiC microcellular foam reinforced aluminium. At low temperature, these composites agreed with those produced here in that their CTE was close to the elastic lower bound; however upon heat-up, their CTE fell, to a value even lower than that predicted by Turner's analysis. This was attributed to the influence of small uninfiltrated voids along narrow crevices in the reinforcement surface. The present composites were infiltrated with pressures an order of magnitude higher than that which was used to produce SiC foam reinforced aluminium composites in [13], (these were produced by gas-driven pressure infiltration). Therefore, it is plausible that far fewer uninfiltrated voids were present in the composites produced in this work, such that the transition observed in [13] is absent.

A smaller decrease in composite CTE as temperature increases, as would be expected to result from the onset of matrix plastic flow in a composite with a fully continuous isotropic reinforcement [13], is not found here either; on the contrary, the CTE seems to increase slightly faster with temperature than do Schapery's elastic bounds. This could be due to incomplete internal bonding of the preforms, leading to the separation of SiC particles across a few areas of particle contact. This would allow some degree of matrix flow around the convex particles to raise the composite thermal expansion upon matrix plastification, as predicted for composites reinforced with a non-percolating reinforcement. This explanation also agrees with the observed gradual character of this transition, since it is quite plausible that some SiC–SiC particle contacts might only open once a certain tensile stress is present across the weaker silica bridges.

Comparison between the theoretical calculations and experimental results for the composites produced without preform oxidation, Fig. 8b, shows that at low temperatures, the composite CTE is near the lower elastic bound, and then features a clear and abrupt increase in the composite CTE near 200 °C, identical with that which was observed with similar composites in [13]. The magnitude of this increase, about $3 \times 10^{-6}\,K^{-1}$, is also similar. We therefore explain this transition analogously, as being due to the combined effects of residual stress and very slight porosity at interparticle contacts, causing an inversion of stresses at interparticle contacts, interparticle separation, and matrix flow around the convex particles at elevated temperatures.

Near 400 °C, the experimental CTE values measured in these composites show an abrupt decrease, and do not agree with any of the theories. Two possible causes, both based on the very soft nature of aluminium at and above 400 °C, can be invoked to explain this transition: (i) slight creep deformation of these composites, under the small load applied by the displacement transducer during the TMA test, and (ii) partial closure of larger voids by local flow of the expanding aluminium matrix.

Overall, this work shows the beneficial influence of percolative particle bonding on the thermal expansion of Al/SiC composites; preoxidation of the particle preforms has prevented the transition in composite CTE towards higher values near 200 °C, thus

lowering, at equal particle loading, the average composite CTE above 200 °C. Since hysteresis in composite expansion is expected to result from this transition [13], the oxidative treatment may also prevent possible thermal ratchetting of components produced with the composites. Finally, we note that bonding of the particles is also likely to increase significantly the resistance of these composites to high-temperature creep; this was probably illustrated in the disappearance of the abrupt decrease in composite CTE which was observed near 400 °C with unoxidized particles.

5. Conclusions

Silicon carbide preforms can be modified by oxidation in air for a few hours at 1300 °C. This treatment produces the formation of a layer of silicon oxide on the particles, which bonds the particles together and confers strength to the preforms. Additionally, this treatment increases the total volume fraction ceramic phase in the preforms, from about 47 to 55 vol %. These preforms can be infiltrated with pressurized molten aluminium by squeeze casting, to produce pore-free composites essentially free of interfacial reaction and preform deformation.

The thermal expansion of squeeze-cast Al/SiC composites produced using oxidized, and non-oxidized, preforms is compared, varying the average SiC particle size from 3 to 40 μm. It is shown that pre-oxidation of SiC preforms, and the interparticle bonds it produces in the composite, eliminates two transitions that are observed as temperature increases in the composite CTE with unoxidized particles. The first transition, which occurs near 200 °C, is explained as resulting from an inversion of stresses at interparticle contacts. Its elimination reduces the composite CTE at elevated temperatures, and prevents hysteresis in composite thermal expansion at high temperatures. Additionally, composites produced in this work show a decrease in their CTE with decreasing particle size; we propose that with oxidized particles, this size dependence is partly due to the low-CTE layer of silicon oxide at their surface.

Acknowledgements

We gratefully acknowledge the support for this work from grant number N00014-93-0613, the US office of Naval Research for MIT authors and partial support from the National Science Foundation for the squeeze casting facility used in this work. We also thank Mr Douglas Matson, Mr Arvind Sundarrajan, and Ms Elisabeth Earhart for assistance and advice with the experimental section of this work.

References

1. D. J. LLOYD, *Inter. Mater. Rev.* **39** (1994) 1.
2. S. ELOMARI, R. BOUKHILI, M. D. SKIBO and J. MASOUNAVE, *J. Mater. Sci.* **30** (1995) 3037.
3. R. J. ARSENAULT, *Scripta Metall.* **22** (1988) 767.
4. Y. FLOM and R. J. ARSENAULT, *J. Metals* **38** (1986) 31.
5. F. A. GIROT, J. M. QUENISSET and R. NASLAIN, *Comp. Sci. Tech.* **30** (1987) 155.
6. R. H. JONES, C. A. LAVENDER and M. T. SMITH, *Scripta Metall.* **21** (1987) 1565.
7. H. J. HEINE, *Founy Mgmt Tech.* **116** (1988) 25.
8. V. C. NARDONE and J. R. STRIFE, *Metall. Trans.* **18** (1987) 109.
9. K. S. RAVICHANDRAN and E. S. DWARKADASA, *J. Metals* **39** (1987) 28.
10. Duralcan composites casting guidelines, "Duralcan composites–mechanical and physical property, Wrought composites, SI Units", 1992, Duralcan USA, San Diego, CA, USA.
11. M. J. KOCZAK, S. C. KHATRI, J. E. ALLISON and M. G. BADER, in "Fundamentals of metal matrix composites", edited by S. Suresh, A. Mortensen and A. Needleman (Butterworth-Heinemann, Boston, 1993) p. 297.
12. C. ZWEBEN, *JOM* **44** (1992) 15.
13. D. K. BALCH, T. J. FITZGERALD, V. J. MICHAUD, A. MORTENSEN, Y.-L. SHEN, and S. SURESH, *Metall. Trans.* accepted.
14. A. BRANDES, Smithells Metals Reference Book (6th edn. Butterworths, London, 1983) p. 14.
15. F. A. HUMMEL "Phase equilibria in ceramic systems" (Marcel Dekker, New York, 1984) p. 32.
16. N. EUSTATHOPOULOS and A. MORTENSEN, in "Fundamentals of metal matrix composites", edited by S. Suresh, A. Mortensen and A. Needleman (Butterworth-Heinemann, Boston, 1993) p. 42.
17. J. NARCISO, A. ALONSO, A. PAMIES, C. G. CORDOVILLA and A. LOUIS, *Metall. Trans.* **26A** (1995) p. 983.
18. R. J. VAIDYA and K. K. CHAWLA, *Comp. Sci. Tech.* **50** (1994) p. 13.
19. E. SIDERIDIS, *Ibid.* **51** (1994) 301.
20. T. H. HAHN, in "Metal matrix composites: mechanisms and properties", edited by R. K. Everett and R. J. Arsenault (Academic Press, Boston, 1991) p. 329.
21. R. A. SCHAPERY, *J. Comp. Mater.* **2** (1968) 380.
22. M. OLSSON, A. E. GIANNAKOPOULOS, and S. SURESH, *J. Mech. Phys. Solids* **43** (1995) 1639.
23. Z. LI and R. C. BRADT, *Int. J. High Technology Ceramics* **4** (1988) 1.
24. Z. R. XU, K. K. CHAWLA, R. MITRA and M. E. FINE, *Scripta Metall. Mater.* **31** (1994) 1525.

Received 20 November 1995
and accepted 13 February 1996